PORT SAID ENGINEERING RESEARCH JOURNAL

Faculty of Engineering - Port Said University
Volume 28 No. 1 pp: 1:15

Numerical study on the stability of marine causeways by using two different geotechnical reinforcement systems of geotextile

*Ahmed Abou Seedah [1 *], Ehab R. Tolba [2], Elsayed M. Galal [3]*

[1*] *Department of Civil Engineering, The High Institute of Engineering and Technology in New Damietta, Damietta, Egypt, email:* a.abouseeda@eng.psu.edu.eg,

[2] *professor, Faculty of Engineering, Port Said University, Port Said, Egypt, email:* prof.tolba@ eng.psu.edu.eg,

[3] *professor, Faculty of Engineering, Port Said University, Port Said, Egypt, email:* elsayed.galal@eng.psu.edu.eg

*Corresponding author, DOI:10.21608/PSERJ.2023.238520.1262

Received 23-9-2023

Revised 24-11-2023,

Accepted 30-11-2023

ABSTRACT

In recent decades, geotextile has been widely used in coastal and geotechnical applications. The main purpose of using it is to achieve higher stability for structures of conventional systems. This paper is mainly concerned with studying the stability of a marine causeway using two different proposed geotechnical reinforcement systems. The first system is a geotextile layers reinforcement system (GLRS), which comprises geotextiles as separated layers embedded in the causeway. The other system is a geotextile mats reinforcement system (GMRS), which differs from the first system in using geotextile as mat units to contain the soil in a closed system. Another purpose of this study is to have a more comprehensive view of the behavior of these systems in three different geotechnical environments, i.e., dense sand as a frictional soil, stiff clay as a cohesive soil, and silty sand as a frictional-cohesive soil. To achieve all of the purposes mentioned above. A numerical study was conducted utilizing finite element software, specifically ABAQUS V6.14. The numerical study was carried out in four main groups: the verification model, the reference models, the (GLRS) models, and the (GMRS) models. During the verification phase, a numerical model was developed to replicate a laboratory test performed on a small-scale geocell-reinforced embankment. In the third and fourth groups, the investigation expanded to include the parametric analysis phase in sequential models to examine each system's parameters that may influence the performance of a marine causeway. The results obtained were compared with those from the second group of reference scenario models. The parametric study of the (GLRS) shows that geotextile thickness is the most obvious parameter of the stability of the causeway. Also, the results confirm that less vertical spacing between layers gives a higher degree of stability; furthermore, the relative length of the geotextile layer does not always need to achieve the maximum value to have an evident effect; it depends on the soil type. Also, it can be concluded from the results that the same parameters function similarly for the other system (GMRS). On the other hand, the results show that the (GLRS) is the more effective system for enhancing the stability of the dense sand marine causeway, while (GMRS) sounds more effective for silty sand soil.

Keywords: Numerical modeling, Marine causeway, Geotextile, Reinforced soil, ABAQUS

1. INTRODUCTION

In the past, using geotextile materials in coastal engineering was limited to working as a filter to retain the excessive migration of the subsoil particles and save the marine structure against scour. In recent decades, these materials have had a new additional role in the coastal field as a tool for geotechnical reinforcement. The last role gained great success in many coastal structures. Many researchers, such as [1], [2], and [3], recommended that embankments need geotextile as reinforcement material to have more stability for their slope. Furthermore, utilizing these materials serves to augment the mechanical and structural characteristics of the soil maintained within quay walls. It was proved that quay walls had become more mechanically stabilized structures, as recommended by [4], [5], and [6].

Geotextiles as a geotechnical reinforced system could be utilized in unprotected or protected structures in marine environments. For unprotected structures, the main considerations are wave impact, wave reflection, and submergence. On the contrary, the main consideration when studying protected structures is submergence. The study in this paper deals with soil reinforcement to enhance the stability of a marine causeway as a sheltered structure; therefore, the primary focal point in the structure mentioned above relates to the impact of submergence on the properties of the reinforced soil.

By using a large direct shear test in an undrained case to examine the shear strength behavior of dry and submerged reinforced sand, [7] concluded that the submerged yielded greater shear strength due to the positive pore pressure. Also, the same result was gained when studying the impact of moisture content on the shear strength behavior of reinforced blocks, which was examined by [8]. In this context, the amount of present water significantly impacts the shear strength. So, it was advised to use clean granular soil or uniformly broken stones as a backfill for submerged walls. [9] came to the conclusion that the submerged sand may show greater shear strength. However, the submerged cohesionless soils in a drained field have the same shear strength as the dry soil.

Regarding geotextile material. [10] have proved experimentally that woven geotextile has a significant influence on the mechanical properties of calcareous sands, which are considered an important material in marine constructions; they made a series of consolidated-drained tests. Their findings show that the strength of the reinforced specimens increases markedly compared to the unreinforced calcareous sand, and the deviatoric stress-strain curves change from slight softening to hardening and dilatancy. Also, by increasing the number of woven geotextile layers and applying a confining pressure, the shear deformation shifts toward strain-hardening behavior. Overall, woven geotextiles significantly improve the apparent cohesion strength of calcareous sand soil. The woven geotextile, relative density, and confining pressure all contribute to volumetric changes and dilatancy of reinforced specimens, but particle breakage is more affected by confining pressure.

Aside from the effect of submergence, many parameters associated with these structures need to be investigated to know their effect on stability. Although field experiments lead to real results, they are considered ponderous, expensive, labor-intensive, and time-consuming. Alternatively, numerical methods are considered the best alternate technique to avoid the abovementioned obstacles of the experimental one. Numerical modeling can recreate the behavior of the studied structure as well as the intricate interactions between the various components of its environment. In the presence of water, this interplay is considered to be more complicated. Furthermore, numerical modeling makes it simple to run several scenarios for the study with varying designs, configurations, and materials. But first, one must ensure the correct use of that approach.

2. METHODOLOGY

ABAQUS V6.14 is the FE modeling program used to investigate the effect of adding two different geotextile systems in a 1:1 slope causeway to improve its lateral displacement. This investigation was carried out in four main models: the first was created to verify a finite element model (FEM) with an experimental model (EM), and the second represents a reference model to study the causeway's stability without adding any reinforcement. The third group of models studied the ability of (GLRS) to enhance the stability of the causeway, and the last group evaluated the enhancement of its stability in the existence of (GMRS).

As available information is scarce on the reinforced marine causeways, the verification step introduced by the first main group is essential; this step exploited the laboratory-tested model of geocell-supported earth embankment presented by [11] to check that FE models running sufficient acceptance. The embankment in the above research was chosen due to the similarity in shape, in addition to the similarity in the main idea of using geosynthetic material in a geotechnical reinforcement approach. Then, the numerical study was extended to obtain lateral displacements on the models of the concerned causeway, which is subjected to surcharge load and hydrostatic pressure from the surrounding seawater, without using any geotextile system as reference results. After that, a number of models were conducted for (GLRS) and (GMRS) to make the parametric studies to evaluate the influence of vertical spacing, geotextile thickness for each system, and relative length for (GLRS). While displaying previous results, a comparison between the performance of each system in the three studied types of soil was conducted. Furthermore, determining which of those systems is more suitable for each type of soil.

3. MODEL SETUP

3.1. Verification model

[11] conducted experimental tests on an embankment reinforced with different geocell types. In this paper, one of these tested embankments is simulated by ABAQUS V6.14 to validate the numerical model by comparing the performance of the simulated model with the experimental observations.

According to their description, they constructed their model with clayey sand embankment soil laid over a soft clay foundation. The reinforcement was a geocell layer located under the embankment's base. Four different geocell types were tested to determine their properties according to standard wide-width strip tension tests (ASTM D 4595) before being employed in the study. The experiment was carried out in a steel tank with dimensions of 1800×800×1200 mm. A 400 mm high embankment with a 45-degree slope and 700 mm crest width was formed over a 100 mm thickness layer reinforced by geocell. The geocell layer was formed by placing several transverse and diagonal strips filled with the same soil of the embankment. The plane view dimensions of the foundation soil of the model were 1800 mm x 800 mm with 600 mm in height to suit the tank dimensions. The experimental model is shown in Figure 1.

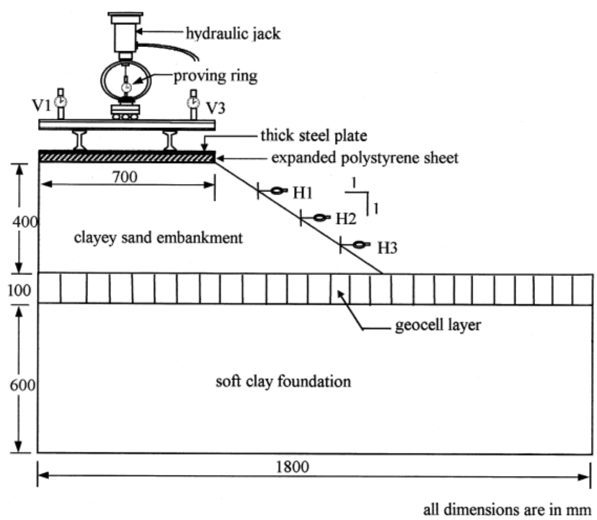

Figure 1: geometry and setup of the experimental model [11]

In this context, [12] exploited that experimental study to perform a simplified 2D model to conduct a parametric finite element analysis using (GEOFEM) program developed at the Royal Military College of Canada. That 2D model depended on an equivalent method to evaluate geocell layer stiffness, owing to not being allowed to simulate it in the 3D model then. That study presented an adequate definition for the constitutive soil model.

In precisely the same fashion as those mentioned above in the 2D numerical model, the soil of the embankment and the subsoil are defined in the 3D model in the present study. All types of soils were modeled using a nonlinear elastic-plastic constitutive model with Mohr-Coulomb (MC) yield criterion and the associated flow rule. Due to its simplicity and extensive usage in geotechnical applications, this model is frequently employed.

According to [13] and [14], this simple constitutive model provides workable findings in the pre-failure scenario. The type of geocell used in this set of experiments is a polypropylene biaxial geogrid having an ultimate tensile strength of 20 kN/m. The (MC) parameters of the embankment, geocell filling, foundation, and BX geocell material are summarized in Table 1 and

Table 2.

4-Node linear tetrahedron finite elements (C3D4) were chosen to soil parts of the numerical model. This element is the 3D mesh of the 2D triangular mesh; triangular elements were reported to be accurate in predicting limit load problems. [15] and [16] reported high success using this mesh arrangement to simulate many reinforced soil embankment problems. 2-Node linear 3-D truss finite elements (T3D2) were used for the geocell parts. Indeed, geocell materials used in geotechnical reinforcement are only subjected to tensile loads. Therefore, they modeled as truss elements. Several meshing sizes were tried to reduce the mesh sensitivity and reach acceptable results insofar as possible. That study is not displayed in the present paper to avoid prolongation. Finally, the mesh was refined up to 64,740 linear tetrahedral elements of type C3D4 for soil parts. At the same time, 2,012 linear line elements of type T3D2 were chosen for geocell parts. An acceptable aspect ratio of less than 2.00 was chosen for the mesh elements.

Table 1. Input parameters for soil in verification model.

Part	Embankment & Geocell Filling	Foundation
Unit weight (KN/m^3)	19	17
Modulus of elasticity (kPa)	25E3	21E3
Poisson's ratio	0.3	0.45
Internal friction angle (degrees)	30	0
Cohesion (kPa)	10	10

Table 2. Input parameters for geocell in verification model.

Density (Kg/m^3)	200
Modulus of elasticity (KPa)	2.63E6
Poisson's ratio	0.33
Opening Size	35 mm × 35 mm

Geocells were defined as components that could be implanted in the soil without slipping to ensure an equal deformation for their nodes [17].

The boundary conditions of the sides and faces of the soil (vertical surfaces) were only prevented from moving in its perpendicular direction. Contrarily, the bottom of the model was fixed in three directions: X, Y& Z; it must be mentioned that the three directions are mentioned as 1, 2, and 3 for results symbols in ABAQUS V6.14 software, respectively. These boundary conditions are usually employed in geotechnical simulation as recommended by [18] and [19]. Figure 2 displays the meshing elements, colored depending on the soil type, in addition to the defined boundary conditions. Figure 3 depicts the geocell elements located directly under the embankment; soil was displayed transparently to show geocell material.

The results of lateral deformation of the numerical model were compared with the results of the laboratory model against the applied surcharge pressure. The outcome, which is mainly involved in the present investigation, is lateral displacement. In ABAQUS V6.14, the lateral displacement is referred to by U1, according to the arrangement of the axes system shown in Figure 2. Three distinct points, H1, H2, and H3, were created in the centerline of the numerical model to represent the positions of the three horizontal displacement gages, cf. Figure 1.

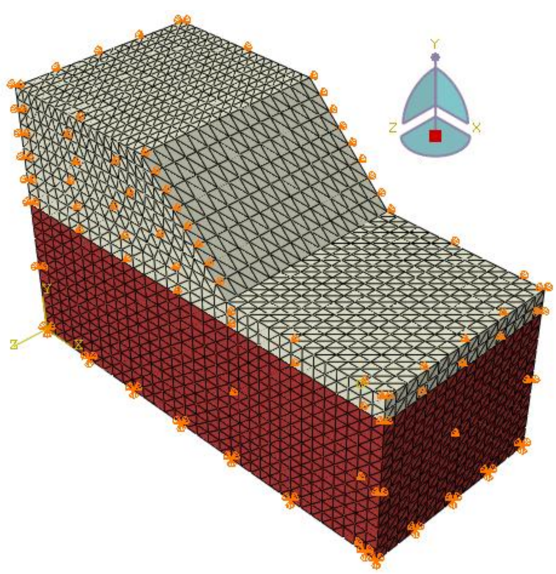

Figure 2: finite elements mesh and boundary condition of the verification model

In Figure 4, the FE modeling results are in sufficient agreement with the laboratory results. However, there may be a discrepancy between the two models since the local compaction impact wasn't taken into account in the numerical modeling. The largest horizontal displacements from the numerical model barely went above 11.0 mm. At the same time, the maximum from the experimental model was 10.48 m at the position of the H3 gauge. Figure 5 illustrates the results of the finite element model in a contour form.

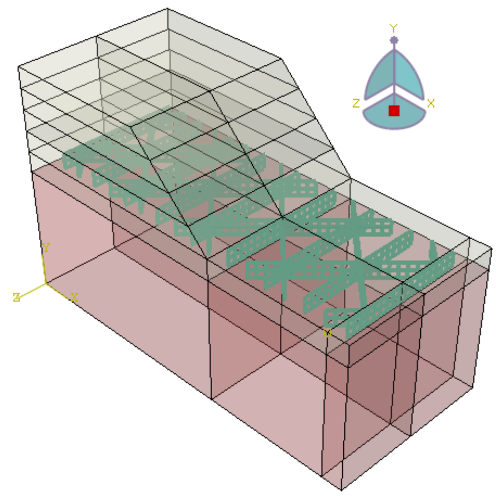

Figure 3: mesh elements for the embedded geocell reinforcement in the verification model

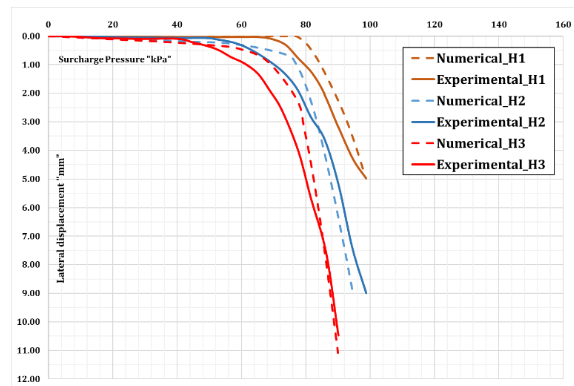

Figure 4: comparison of lateral deformation obtained from the EF model and the experimental measurements.

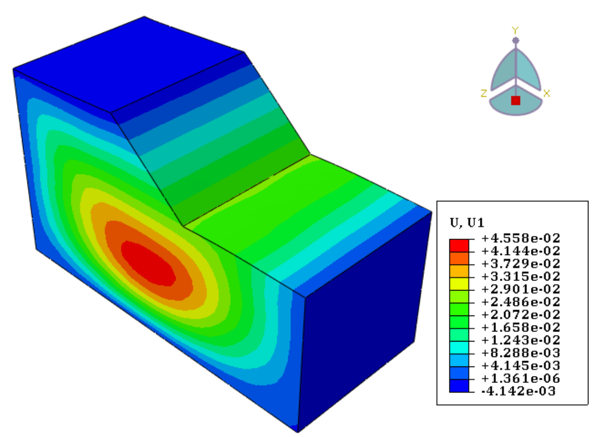

Figure 5: contoured results of lateral displacement in the verification model

3.2. Reference models

Models in this section were created to have reference values for the deformation results before adding any geotechnical reinforcement. A complete configuration of the marine causeway with a 4.00 m height, 8.00 m crest width, and 1:1 side slope is shown in Figure 6. These dimensions were chosen to give a small margin of safety within the slope stability study. The soil of the causeway and its foundation were chosen to be the same. However, three different categories for the soil were chosen, i.e., Dense sand, silty sand, and stiff clay. The soil was modeled using the same model used in the previous section, the Mohr-Coulomb constitutive model; values of soil parameters are displayed in Table 3.

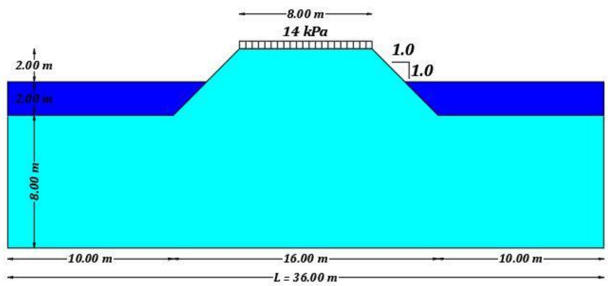

Figure 6: typical cross-section of the marine causeway "Reference Model"

Table 3. Input parameters for soil in FE models.

Type of Soil	Unit	Dense Sand	Silty Sand	Stiff Clay
• General				
Dry unit weight	KN/m³	16.5	17.8	18.67
Submerged unit weight	KN/m³	9.50	10.8	11.67
• Elasticity				
E: Modulus of Elasticity	pa	75E6	19.6E6	60E6
υ: Poisson's ratio	-	0.35	0.3	0.45
• Plasticity				
Ø: friction angle	Degree	38	25	0
Ψ: Dilation angle	Degree	8	0	0
C: Cohesion	pa	1E3	24E3	150E3
Reference		[20]	[21]	[20]

Before investigating FE models for the concerned causeway, the initial slope stability was studied by Limit Equilibrium Methods (LEM) using "Slide_Rocscience V6" software. Table 4 displays the results obtained for safety factors by three different methods for each soil type. Figure 7, Figure 8, and Figure 9 show potential failure surfaces and detailed results for (FOS) for the three studied soil types of the causeway. Values of (FOS) showed that dense sand causeway has the minimum margin of safety compared with the other two types. The author preferred to set the same dimensions for all soil types to make a fair judgment for the results of using the proposed geotechnical systems with a simple comparison.

Table 4. Results of slope stability analysis .

Soil Type	FO S		
	Spencer	Bishop simp.	GLE/Morgen.
Dense Sand	1.09	1.10	1.09
Silty sand	2.94	2.97	2.94
Stiff clay	11.20	11.20	11.20

The causeway section used in the FE analysis is 6.00 m in length, representing part of the causeway's longitudinal direction. Boundary conditions and finite element mesh were the same as used in the verification model section. No movement was allowed for the base of the foundation in the three directions, while the vertical ends of the modeled causeway were restricted from movement within their own plane. Again, 4-Node linear tetrahedron finite elements (C3D4) were used for the finite elements mesh.

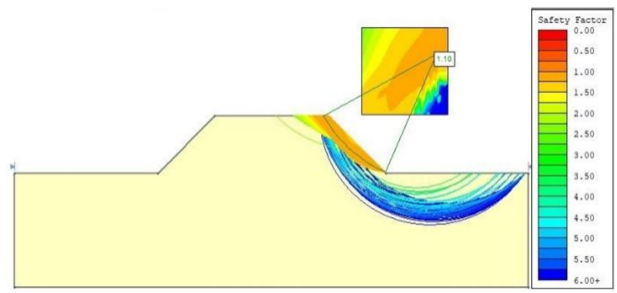

Figure 7: failure surfaces and detailed results for Safety Factor in dense sand causeway

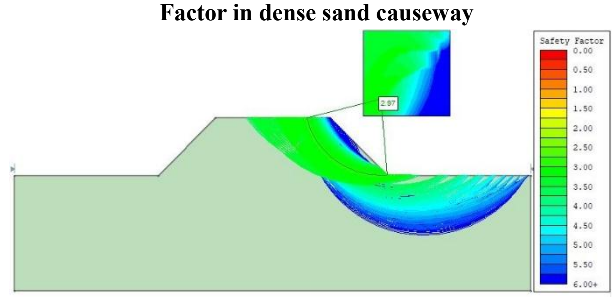

Figure 8: failure surfaces and detailed results for Safety Factor in silty sand causeway

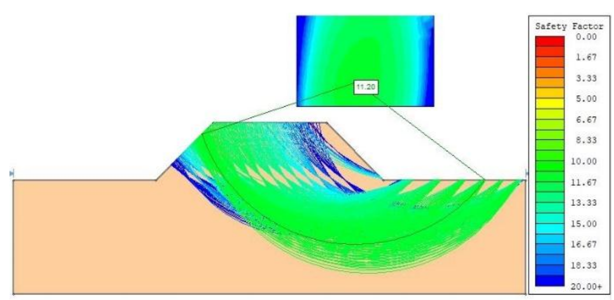

Figure 9: failure surfaces and detailed results for Safety Factor in stiff clay causeway

Besides the self-weight of the causeway, a surcharge pressure of 14 kPa was applied on the crest surface of the causeway, which represents a two-lane road structure according to Standard Specifications for Highway Bridges [22]. A hydrostatic load representing a water depth of 2.00 m was applied on the two sides of the causeway. Figure 10 shows results for lateral displacement on the right inclined surface of the marine causeway for the three studied soils. The dense sand causeway leads to the smallest lateral deformation with a maximum value of less than 0.5 mm. In contrast, the silty sand model shows the highest ability for lateral deformation among the three types, with a value not exceeding 2.5 mm. The high negative value for the lateral displacement for the silty sand model could be interpreted by the large vertical displacement obtained in that type of soil in comparison to the other types. The vertical displacement was not displayed as it is outside the scope of the present study, which concentrates on lateral displacement.

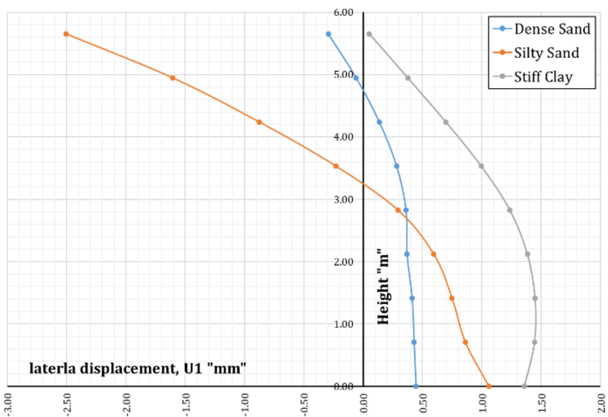

Figure 10: lateral displacement of the marine causeway for the three types of soils

3.3. GLRS models

These models aim to study the degree of enhancing the stability of the concerned marine causeway by adding a group of separated geotextile layers as a kind of geotechnical reinforcement. This technique is usually used in retaining walls such as (GRS) walls. This investigation is considered a try to find a new application for this material as a reinforcement in a marine causeway. These models are simulated with the same loads, boundary conditions, and soil materials used in the reference models in the previous section, except that the new part, geotextile layers, has been added as an embedded part in the soil. Figure 11 shows the proposed Geotextile Layers Reinforcement System (GLRS) in this investigation.

The geotextile layers are parts that offer strength in the plane of the surface without bending stiffness. Therefore, linear integration shell elements were assigned to the linear elastic material. Mesh was chosen within a 1:1 aspect ratio, with linear quadrilateral shell elements (S4R) of reduced integration elements to save computation time during the simulation. The length for each geotextile layer (L) was stated to be suitable for the width of the causeway (B) at the level of placement according to the desired relative length (L/B). The material parameters of the geotextile were in line with Table 5 [23] and [24].

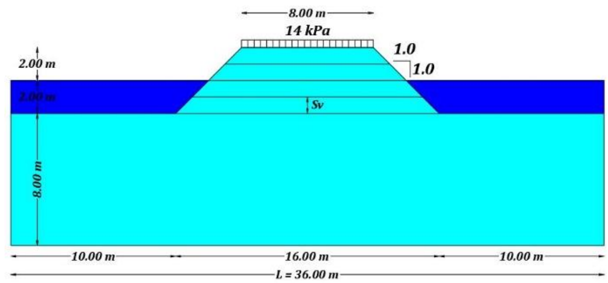

Figure 11: purposed Geotextile Layers Reinforcement System "GLRS" for the marine causeway

For parametric study purposes, three different parameters were considered in this system: vertical spacing between the geotextile layer (S_v), the thickness of the geotextile layer (t), and the relative length of the geotextile layer (L/B). For each parameter, three different values were assumed. For the judgment on the (S_v) effect, three values were investigated: 0.5, 1.00, and 2.00 m. Furthermore, three thicknesses are studied: 3.00, 6.00, and 12.00 mm. At the same time, values of (L/B) were 0.50, 0.75, and 1.00.

Table 5. Input parameters for geotextile material.

Density (Kg/m^3)	75
Modulus of elasticity (KPa)	7.035E6
Poisson's ratio	0.45
Thickness (mm)	3

During (GLRS) modeling, some assumptions were considered: the capacity of geotextile strength is adequate for the generated straining stresses on it, the impact of seams and its strength were neglected during simulation, and scour in the surrounding soil and creep effects on the geotextile material were not taken into consideration.

3.4. GMRS models

These models aim for the same purpose as the previous system with a new technique. The system under explanation in this section is the geotextile mats reinforcement system, denoted as (GMRS). An attempt to use the geotextile material in a new scheme, which depends on using closed units of geotextile skin, the units can be implemented by the placement of geotextile layers in-site and forming a filling core of soil with the desired height and dimensions, then, the layer is covered again with the same geotextile skins and sewn together to form a closed mat. The same loads, Boundary conditions, soil materials, and FE mesh used in the (GLRS) models are used again in this system.

For parametric study purposes, only the height of the geotextile mat (H) and the thickness of the geotextile skin (t) were investigated. Again, for each parameter, three different values were assumed. For the judgment on the (H) effect, three values were investigated: 0.5, 1.00, and 2.00 m. Furthermore, the same thicknesses in the previous system were studied in this system. Figure 12 shows the proposed geotextile mats reinforcement system (GMRS).

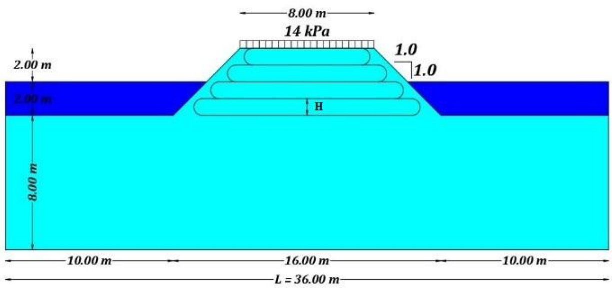

Figure 12: purposed Geotextile Mats Reinforcement System "GMRS" for the marine Causeway

4. RESULTS AND DISCUSSION

4.1. Effect of geotextile layers reinforcement system (GLRS)

With a single alteration in each run, several models were produced. To understand the effect of each parameter for this suggested system (GLRS) on the deformation of the concerned marine causeway, the following sub-sections display charts and results for each parameter.

4.1.1. Effect of vertical spacing between geotextile layers in GLRS

Many previous works have studied the effect of vertical spacing between geotextile layers in other marine structures. One of these structures is geosynthetic reinforced structure retaining walls (GRS), which intuitively differs from the presently studied structure. [5], [25] and [14] recommended a small vertical spacing to reduce the presumable deformation for their studied structures; the recommended values were less than 1.00 m. Therefore, in the present study, three models were analyzed with vertical geotextile spacings 0.50 m, 1.00 m, and 2.00 m to explain how vertical spacing affects the marine causeway's lateral deformation.

Figure 13**,** Figure 14**,** and Figure 15 demonstrate the impact of the geotextile's vertical spacing on the resulting lateral deformation at the right side slope of the marine causeway. The three figures show results for the three soils: dense sand, silty sand, and stiff clay. Figures show that the effect of the vertical spacing concentrates on the lower two-thirds and diminishes for the upper third, especially in the dense sand and stiff clay models. In contrast, the effect shows a nonuniform performance along the upper and lower half of the inclined surface of the silty sand model.

Consequently, it could be easily recommended to use smaller vertical spacing for GLRS, which enhances the lateral displacement, especially for the lower levels of the marine causeway. In Figure 13, results show that the maximum U1 in the dense sand model was 0.44 mm at the toe point for the non-reinforced model; this point reached non-far values for the three studied vertical spacing of the other reinforced models, with the smallest value of about 0.42 mm belonging to the 0.50 vertical spacing system. Aside from the toe point, the influence of "GLRS" looks more effective near the mid-height of the causeway at the height of 3.50 m, where U1 reaches 0.28 mm for the non-reinforced model. At the same level, it reaches only a value of 0.17 mm for the 0.50 m vertical spacing system.

Contrary to the previous case, the maximum lateral deformation for the silty sand causeway was observed at the crest level with a value of 2.51 mm to the inside direction, as shown in Figure 14. This value is approximately fixed for the non-reinforced model and 1.00 & 2.00 m (S_v) reinforced models. In comparison, that value was only about 2.02 mm, with an enhancement percentage of about 19.57 % at this level. For the last type of soil shown in Figure 15, the maximum U1 was observed at level 1.50 m with a value of 1.45 mm for the nonreinforced system; the decrease in this value undoubtedly happened for the proposed reinforced models with values of 1.36, 1.28, and 1.17 mm for the descending order vertical spacing systems.

Figure 16 shows the U1's maximum enhancement percentage for all studied models along the right-side inclination surface. The maximum enhancement percentage was calculated by estimating the enhancement percentage at each node along the right side slope, 9 nodes, and then taking the maximum value. For each node, the value could be calculated by estimating the percentage of dividing the difference between the reference model result and the present model result on the reference model. Results obtained from the three types of soils show that small vertical spacing between geotextile layers is always required for a higher degree of stability. This result could be interpreted as follows: choosing small vertical spacing between geotextile layers gives more geotextile layer numbers, which allows a greater number of friction interaction planes between geotextile layers and the surrounding soil. Thus, more stability for the marine causeway could be achieved. It is worth mentioning that using GLRS shows a higher degree of effectiveness in the dense sand than the other two types; this finding could be mainly due to the internal friction angle, which has a high value in that model.

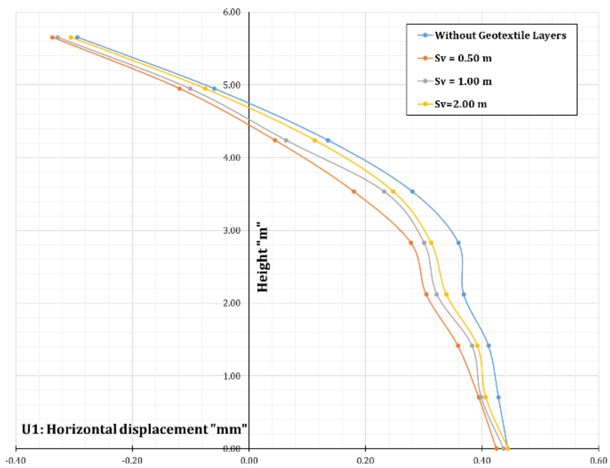

Figure 13: U1 of the dense sand marine causeway for different geotextile layer's vertical spacings in (GLRS)

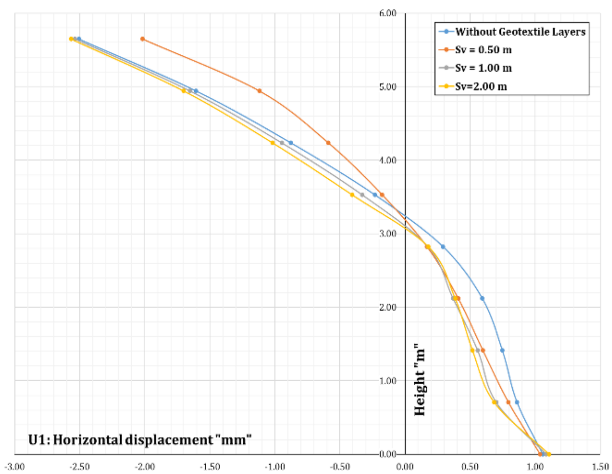

Figure 14: U1 of the silty sand marine causeway for different geotextile layer's vertical spacings in (GLRS)

4.1.2. Effect of geotextile thickness in GLRS

In this context, Figure 17, Figure 18, and Figure 19 illustrate the influence of another parameter, i.e., the thickness of geotextile layers. Three different thicknesses are studied for this purpose: 3.00, 6.00, and 12.00 mm; practically, composite double-separated layers could achieve the last thickness. The vertical spacing between geotextile layers was fixed at 0.50 m for all studied models in this sub-section. Figures show the lateral deformation of the right side slope of the causeway for the three studied types of soils. Remarkably, the thickness of geotextile layers could be considered a key role parameter. Increasing the thickness could dramatically increase the stability of the marine causeway. The author interprets that result as the greater the thickness of layers, the greater the ability to endure normal stresses. So, it could be concluded that maximum thickness is an important choice for designing (GLRS). Again, Figure 20 states that (GLRS) has the highest influence in the dense sand causeway, with a maximum value of 96.38%. The low rigidity against lateral displacement shown in Figure 10 could interpret the small values reached in Figure 20 for the silty sand model, which means that the obtained decrease in the lateral displacement by the proposal system is not sufficient to cover the high values of the lateral displacement in the reference scenario. However, an additional high capacity to resist lateral displacement was achieved in the three types of soil by increasing the thickness of geotextile layers.

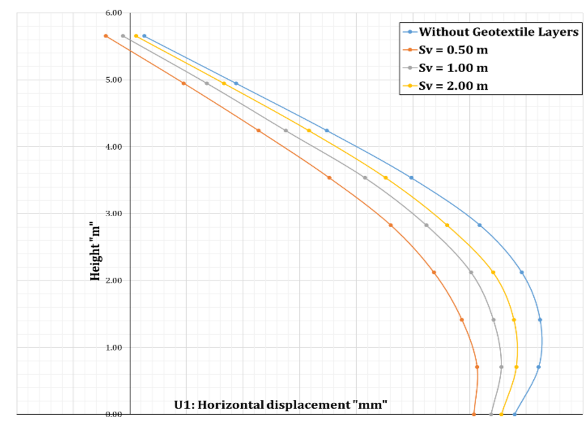

Figure 15: U1 of the stiff clay marine causeway for different geotextile layer's vertical spacings in "GLRS"

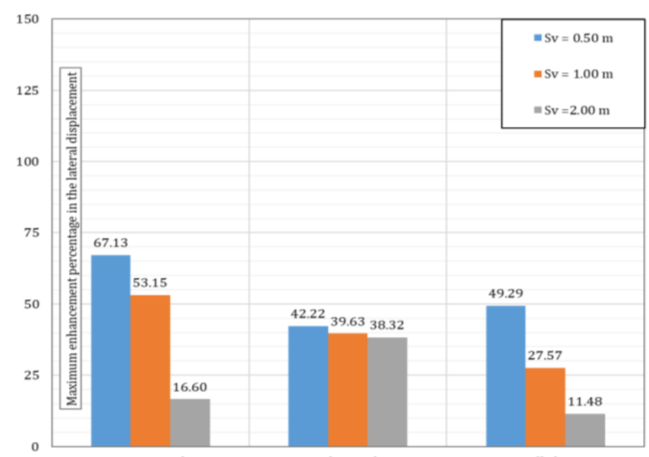

Figure 16: Percentage of maximum enhancement in the lateral displacement of the three types of soil for different geotextile layer's vertical spacings in "GLRS"

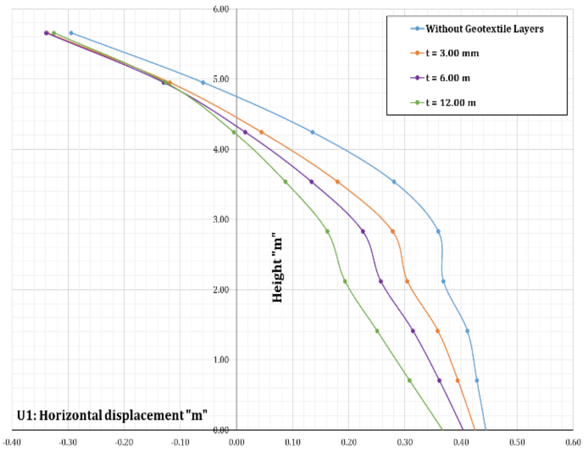

Figure 17: U1 of the dense sand marine causeway for different geotextile thicknesses in (GLRS)

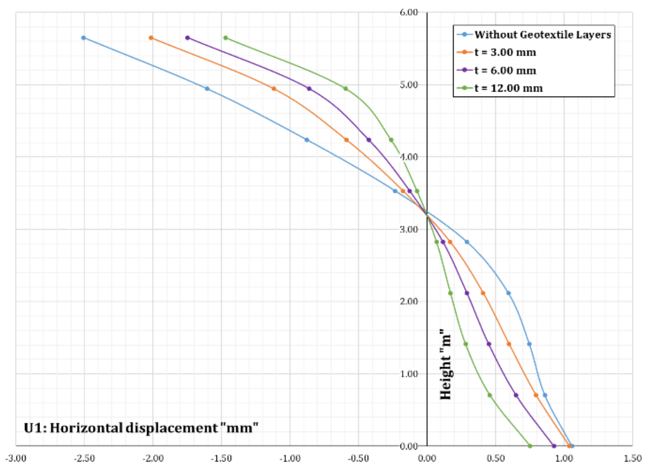

Figure 18: U1 of the silty sand marine causeway for different geotextile thicknesses in (GLRS)

4.1.3. Effect of geotextile relative length in GLRS

Three different relative lengths were examined in this study as follows: (L/B) = 0.5, 0.75, and 1.00. As mentioned before, L represents the length of the geotextile layer in the desired level, while B is the width of the causeway at the same level. In all models studied in this section, the thickness of geotextile and vertical spacing between geotextile layers were fixed to be 3.00 mm and 0.50 m, respectively. To assess the influence of that parameter. It must be mentioned here that all models in all previous sections had a complete relative length.

Figure 21, Figure 22, and Figure 23 show the results of lateral deformation for the three studied types of soils to evaluate the influence of the relative length of the geotextile layer. The results of dense sand and silty sand models, which are shown in Figure 21 and Figure 22, respectively, demonstrate that the behavior of that parameter differs along the height of the causeway, where the unity value for the relative length gives the best stability in the upper half only, while, the same value does not guarantee the best stability for the lower half. However, for the lower half results, the 0.75 relative length gives the lowest lateral displacement in the dense sand causeway. In contrast, the half value has the more rigid behavior in the silty sand one. The superiority of the noncomplete relative length models in the lower half could be explained by the absence of a cutting plane, which gives a chance for more integration between soil particles. However, the difference in results found for this parameter is not as clear as the two previous parameters, which sound to be more effective in the designing process of that system (GLRS).

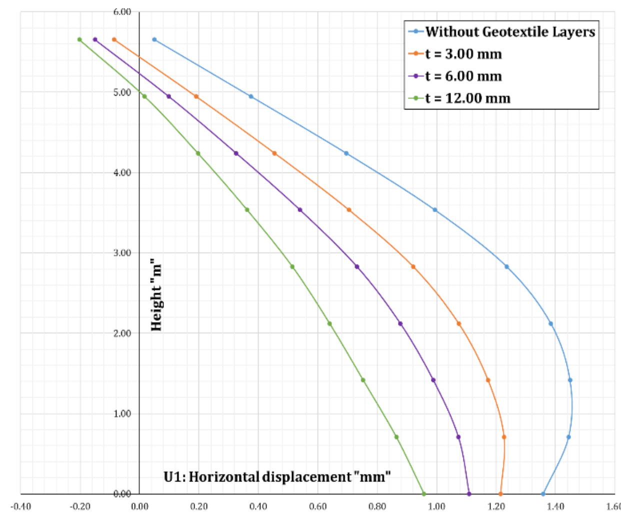

Figure 19: U1 of the stiff clay marine causeway for different geotextile thicknesses in (GLRS)

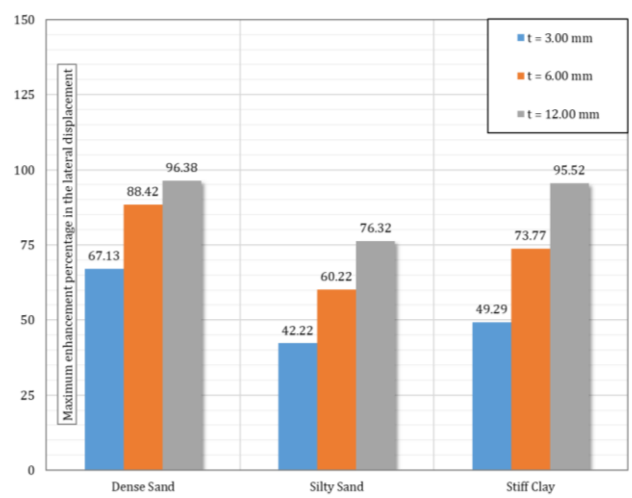

Figure 20: percentage of maximum enhancement in the lateral displacement of the three types of soil for different geotextile thicknesses in (GLRS)

On the other hand, for the stiff clay causeway in Figure 23, lateral displacement appears to have a consistent behavior along the whole height of the causeway; results show that greater (L/B) mean smaller lateral displacement; however, results of (L/B) equal

0.75 and 1.00 give very close values, that gives the designer the possibility to not always choose the complete relative length for the geotextile layers in (GLRS) in that type of soil. The last results can be interpreted as follows: the 0.75 and 1.00 relative lengths guarantee the crossing of the slip failure circle by the geotextile layers. Figure 9 in section 3.2 shows that the slip circle has a relatively high radius. However, the maximum lateral displacement has been reached at the height of approximately 1.50 m; the value of U1 at this height was 1.45 mm for the non-reinforced model, while the value was 1.17, 1.19, and 1.27 mm for relative length 1.00, 0.75, and 0.50, respectively. The enhancement percentage values for these results are 19.05%, 17.89%, and 12.32% for the three relative lengths in order.

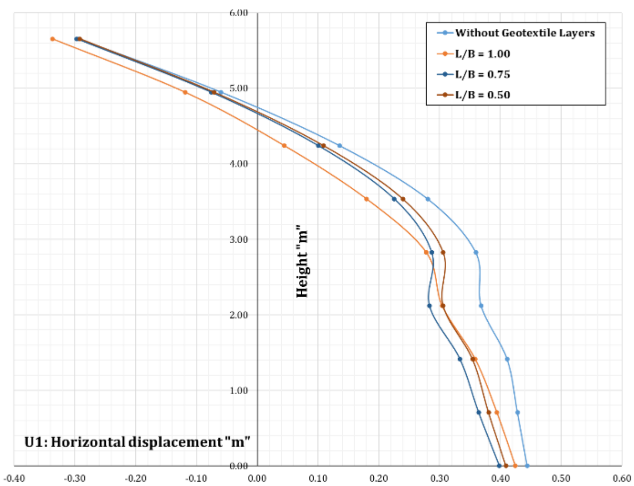

Figure 21: U1 of the dense sand marine causeway, with different relative lengths in (GLRS)

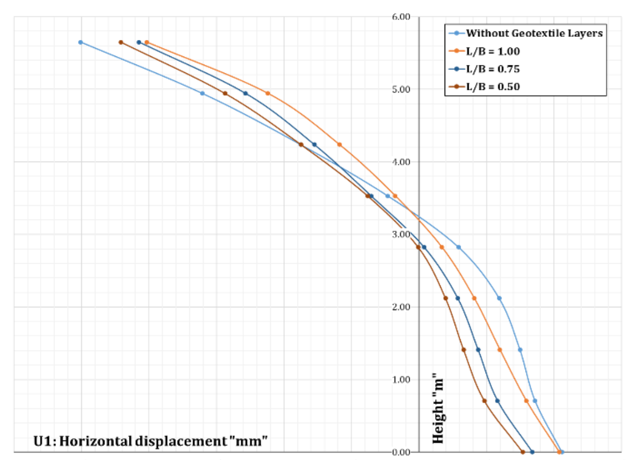

Figure 22: U1 of the silty sand marine causeway for different relative lengths in (GLRS)

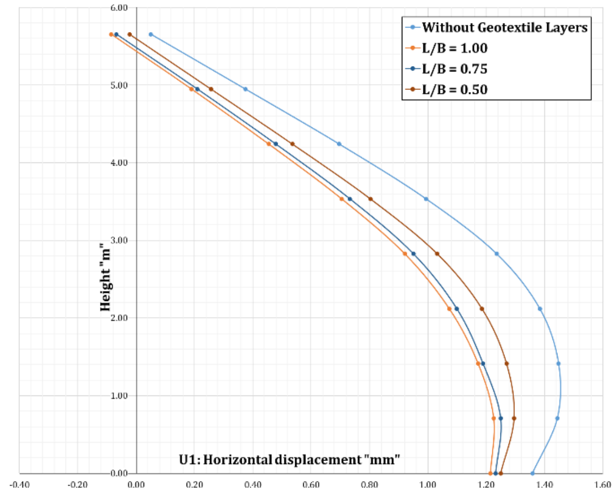

Figure 23: U1 displacement of the stiff clay marine causeway for different relative lengths in "GLRS" effect of the height of geotextile mats in "GMRS."

4.2. Effect of geotextile mats reinforcement system (GMRS).

Numerous models have been created to investigate the performance of (GMRS) and to make its parametric study. Therefore, lateral displacement for the right side slope of the concerned marine causeway will be displayed in this sub-section.

4.2.1. Effect of the height of geotextile mats in (GMRS)

To evaluate the influence of this parameter and compare the lateral displacement results of the concerned causeway for the three types of soils**.** Figure 24**,** Figure 25**,** and Figure 26 are displayed. All results depicted in these models have 3.00 mm geotextile skin thickness as a constant thickness, while the height of mats changed to 0.50, 1.00, and 2.00 m. The length of mats, as shown in the cross-section in Figure 12, was chosen to have a sufficient distance before the inclined surface of the marine causeway to avoid interposition between the results of soil and geotextile material.

Figure 24 shows the lateral displacement for the dense sand causeway; the lateral displacement ranges from the maximum value of 0.44 mm for the reference model to the minimum value of 0.41 mm for the 0.50 m mat height model. Aside from the small difference between the stated values at the toe, Results show a higher degree of influence gained by (GMRS), especially at the level near the mid-height of the causeway, where the value of lateral displacement gained from the reference model is 0.36 mm. In contrast, the values at the same location were 0.27 mm, 0.31 mm, and 0.32 mm for the heights of 0.50 m, 1.00 m, and 2.00m, respectively. Enhancement values accompany these values at this position of 22.68

%, 13.68 %, and 8.73 % for the same three heights in order.

Figure 25 shows lateral deformations of the silty sand causeway. It could be concluded that using a design of a small height mat is required to reach the maximum required enhancement. Screening of U1 values shows that the maximum lateral displacement of this causeway is 2.51 mm for the unreinforced causeway, while a value of 1.66 mm is only reached by the 0.50 m height mat in (GMRS).

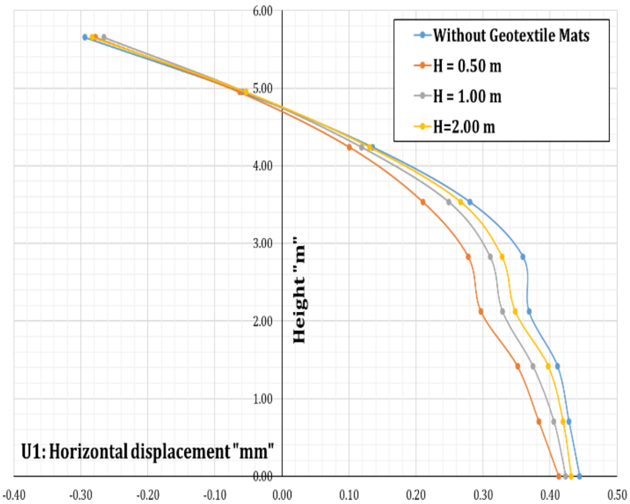

Figure 24: U1 of the Dense sand marine causeway, with different mat heights in (GMRS)

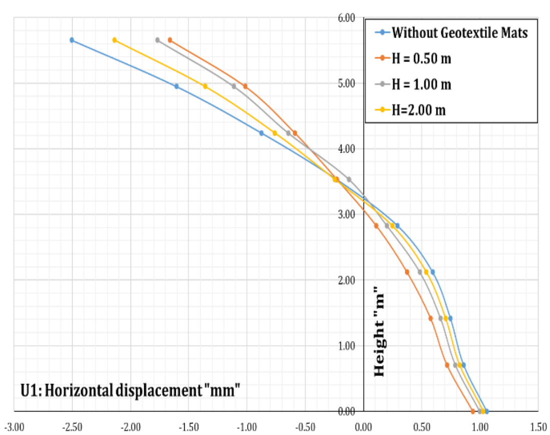

Figure 25: U1 of the Silty sand marine causeway, with different mat heights in (GMRS)

Figure 26 shows the results of the stiff clay causeway. Again, the same conclusion is obtained, which means that a small height mat is an advised criterion. Screening of U1 values shows that maximum lateral displacement of this causeway occurs at the beginning of the lower third of the causeway. A value of 1.45 mm is obtained for the unreinforced causeway, while a value of 1.10 mm is only reached by the 0.50 m height mat in (GMRS).

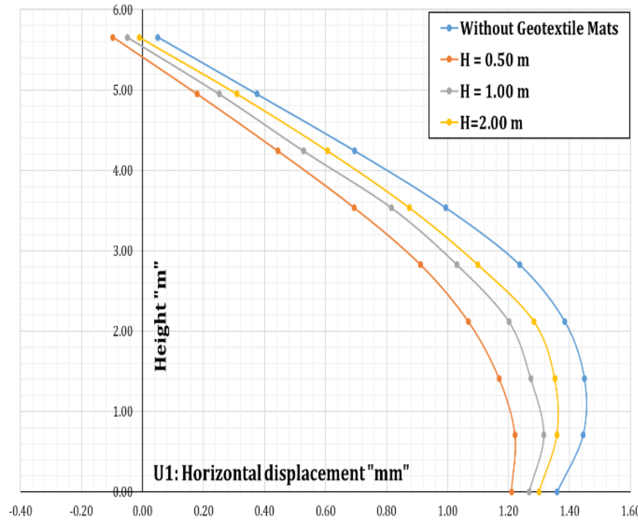

Figure 26: U1 of the Stiff clay marine causeway, with different mat heights in (GMRS)

4.2.2. Effect of skin thickness of geotextile mats in (GMRS).

This subsection studies the effect of the mats' geotextile skin thickness. The results of lateral displacement of the concerned causeway for the three types of soils are displayed in Figure 27, Figure 28, and Figure 29. All models studied in this part have mats that are 0.50 m high. However, the three different thicknesses of the studied geotextile skins are 3.00, 6.00, and 12.00 mm.

Similar to the previous system, it is easily demonstrated that this parameter has a larger influence on the stability enhancement of the concerned causeway than the previous parameter. In Figure 27, the maximum value of U1 is 0.44 for the unreinforced causeway. At the same time, this value becomes 0.41, 0.39, and 0.35 mm for the thicknesses 3.00 mm, 6.00 mm, and 12.00 mm, respectively. Otherwise, these values become 0.36 mm, 0.27 mm, 0.22 mm, and 0.16 mm for the four models, respectively, at the mid-height for the causeway.

The results of the silty sand causeway are shown in Figure 28. The maximum U2 is 2.5 mm for the reference model, while that value is only 1.66 mm, 1.33 mm, and 0.98 mm for the three thicknesses in the ascending order. The result revealed the same behavior for the stiff clay model in Figure 29, where the maximum values are 1.45 mm, 1.7 mm, 0.99 mm, and 0.76 mm for the four displayed models, respectively. The change percentage in this location is 19.30 %, 31.74 %, and 47.31 % for the three thicknesses, respectively. Between all the studied thicknesses in this section, the maximum enhancement percentage is 119.17 for the silty sand causeway.

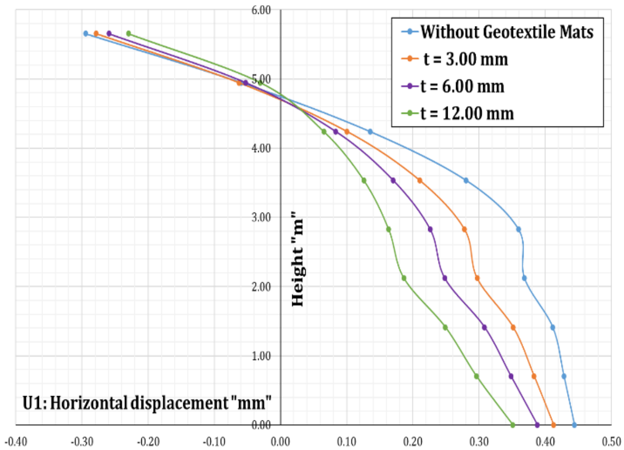

Figure 27: lateral displacement of the Dense Sand marine causeway, with different geotextile skin thickness in (GMRS)

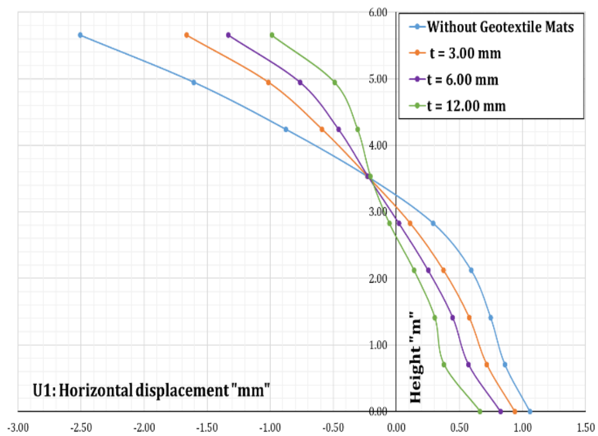

Figure 28: lateral displacement of the Silty Sand marine causeway, with different geotextile skin thickness in (GMRS)

4.1. Comparison between "GLRS" and "GMRS"

This section compares the two suggested systems, i.e., (GLRS) and (GMRS). The results of lateral displacement of the causeway for the three stated soils are displayed in Figure 30, Figure 31, and Figure 32. The thickness of the geotextile for the two systems is chosen to be 3.00 mm, the values of (S_v) and (H)" are 0.50 m, and the (L/B) is unity for the "GLRS."

Figure 30 shows the results in the dense sand soil. The chart ensures that GLRS is the advised system for that type of soil, especially for the upper portion of the causeway; that finding could explain the existence of more friction planes in the GLRS system between the soil and the geotextile layers, especially for being mainly friction soil.

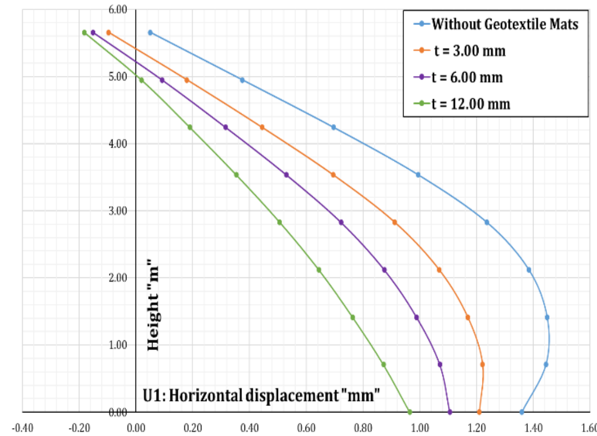

Figure 29: lateral displacement of the Stiff clay marine causeway, with different geotextile skin thickness in (GMRS)

Contrary to the previous finding, Figure 31 shows that GMRS shows a slight leading over the open system. The fact that the silty sand soil is friction cohesion soil gives priority to the GMRS as the closed system appears to provide more rigidity due to the existence of cohesion; at the same time, it gives friction planes between the soil and the geotextile skin.

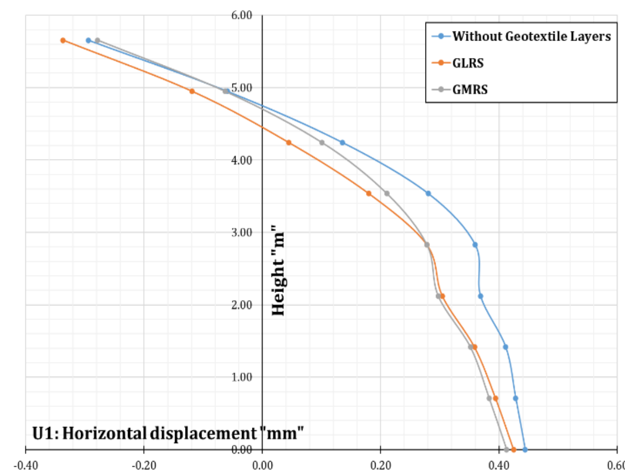

Figure 30: lateral displacement of the Dense Sand marine causeway with (GLRS) and (GMRS)

On the other hand, Figure 32 shows that the two systems give identical performances in the stiff clay medium, which means that the two suggested systems can work in the same manner in the high cohesion soil; that finding could be useful when deciding the easier system for construction, rather than using the closed system (GMRS) which is considered more complicated and less economical.

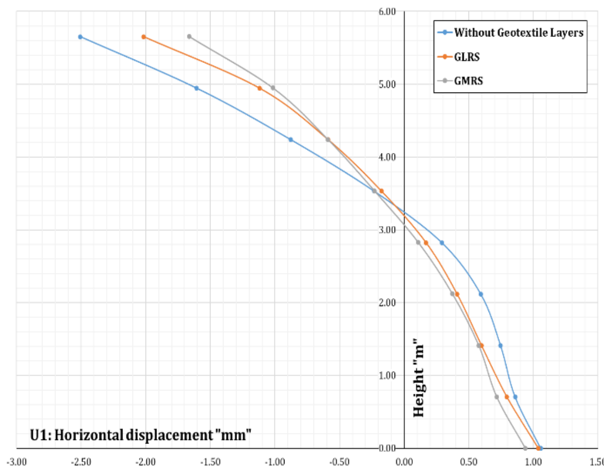

Figure 31: lateral displacement of the silty Sand marine causeway with (GLRS) and (GMRS)

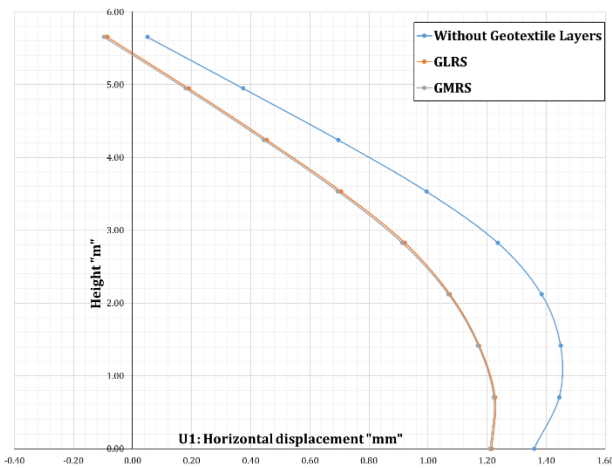

Figure 32: lateral displacement of the stiff clay marine causeway with (GLRS) and (GMRS)

5.CONCLUSION

This study uses an experimental geocell-reinforced embankment to test the validity of a numerical model that could simulate the reinforced embankment's deformation. The numerical analysis was done using the ABAQUS V6.14 program.

After that, the numerical models were extended to three large-scale reference models, which simulate three types of soil: dense sand, silty sand, and stiff clay for the same configuration of marine causeways. The reference models were created to simulate the condition in the coastal environment that might influence the stability of the causeway in the basic case before adding any geotechnical reinforcement systems. Also, at this step, the slope stability analysis by "LEM" using "Slide_Rocscience V6" software is conducted to evaluate the safety factor and indicate the potential position of slip failure.

The next step involved studying two different reinforcement systems; (GLRS) which consists of a number of separated geotextile layers, and (GMRS) which consists of several stacked closed geotextile mats. A parametric study was performed for each system by changing a single parameter in each model to evaluate the lateral displacement of the inclined surface of the concerned causeways. The results of the analyses conducted in this study concluded that:

- The two systems presented could be used as satisfactory techniques to obtain geotechnical reinforcement for marine causeways with sustainability in the recommended construction and design criteria.

- In principle, it could be noticed that, depending on the type of soil, the maximum lateral displacement may occur in different locations on the inclined surface of the causeway; it may occur at the toe of the dense sand causeway, at the crest of the silty sand causeway, and the highest level of the lower third part of the stiff clay causeway. Also, the silty sand obtained the largest lateral deformation, while the dense sand shows a stiffer behavior between the three models.

- The geotextile thickness was found to affect the stability of the causeway for the two presented systems, (GLRS) and (GMRS), highly. The effect of geotextile thickness in the numerical investigation was studied using three different values: 3.00 mm, 6.00 m, and 12.00 m. The most enhancement in the stability of the concerned causeway was obtained when using the 12.00 mm thickness. This thickness may not be common but could be formed by gathering two layers. The maximum enhancement percentage reached by that thickness was 96.38% and 119.17% for the (GLRS) in the dense sand causeway and (GMRS) in the silty sand causeway, respectively.

- For the GLRS, the full relative geotextile length does not always give the best results; that result could be interpreted as follows: for stiff clay, the results of the lateral displacement do not differ much between the two values 1.00 and 0.75. while in the other causeways, i.e., dense sand and silty sand, the maximum decrease in the lateral displacement was not always achieved for the case of L/B =1.00; whatever, this note appears only in the upper half of the causeways and is not extended to the lower portion, while the lower half shows that L/B=0.75 and 0.50 obtain the maximum enhancement of the causeway stability. However, unlike the thickness parameter, the relative length parameter does not show a noncomplex influence.

- For (GLRS), the results of the numerical investigation show that vertical spacing moderately influences causeway deformation compared to thickness. The numerical study in this paper was conducted for vertical spacing equal to 0.50, 1.00, and 2.00 m between geotextile layers. The effect sounds significant in the lower part and fades in the upper part for the dense sand and stiff clay causeways. The best stability appears in the upper part of the silty sand causeway. It is recommended to use a vertical spacing of 0.50 m to obtain a broad enhancement in the stability of the causeway. Also, the same previous value is recommended for the height of mats in GMRS.

- Finally, comparing the results of the same design of both systems shows that (GLRS) could be considered preferable for dense sand. At the same time (GMRS) could be recommended for the silty sand causeway, while both systems have a very similar influence on the stability of the causeway.

6.RECOMMENDATIONS FOR FUTURE WORKS

- Study the effect of the proposed system on other dimensions and slopes of marine causeways.
- Study the effect of compaction and consolidation on the stability of marine causeways during the existence of the proposed systems.
- Study the effect of creep that may occur in the geotextile layers.
- Study the stresses in the geotextile material and the efficiency of seams.
- Studying the stability of the marine causeway in unsheltered areas against wave attack.
- Perform physical modeling in the field to analyze the stability of the marine causeway.
- Study potential failure models, such as sliding, overturning, and stress, that may occur individually under aggressive loading situations.
- Try the proposed systems in other marine structures, such as quay walls.

7. LIST OF SYMBOLS

- GLRS: Geotextile Layers reinforcement system
- GMRS: Geotextile Mats reinforcement system
- FEM: Finite Element Model
- EM: Experimental Model
- LEM: Limit Equilibrium Method
- FOS: Factor of Safety
- MC: Mohr-Coulomb constitutive model
- E: Modulus of Elasticity
- υ: Poisson's ratio
- Ø: Internal friction angle of soil
- C: Cohesion of soil
- Ψ: Dilation angle of soil
- U1: lateral displacement
- Sv: vertical spacing between layers in (GLRS).
- t: thickness of the geotextile layer in (GLRS).
- L/B: the relative length of the geotextile layer.
- L: the length of the geotextile layer in (GLRS).
- B: The width of the causeway at the same level as the geotextile layer in (GLRS).
- t: the thickness of the geotextile skin in (GMRS).
- h: the height of the geotextile mat in (GMRS).

- **Credit Authorship Contribution Statement:**

Ahmed Abou Seedah: Literature review, Methodology, Software, Formal analysis, original draft preparation, and Investigation; **Ehab Tolba**: Visualization, Conceptualization, Supervision, Investigation, and Reviewing; **Elsayed Galal**: Visualization, Conceptualization, Methodology, Original draft preparation, Supervision, Editing, and Reviewing.

- **Declaration of Competing Interest**

The authors declare that they have no known competing financial interests or personal relationships that could have appeared to influence the work reported in this paper.

- **Declaration of Funding**

This manuscript has no funding

8.REFERENCES

[1] Madhavi Latha, G., K. Rajagopal, and N. Krishnaswamy, Experimental and theoretical investigations on geocell-supported embankments. International Journal of Geomechanics, 2006. 6(1): p. 30-35.

[2] Taechakumthorn, C. and R.K. Rowe, Performance of reinforced embankments on rate-sensitive soils under working conditions considering effect of reinforcement viscosity. International Journal of Geomechanics, 2012. 12(4): p. 381-390.

[3] Yapage, N., et al., Numerical modeling of geotextile-reinforced embankments over deep cement mixed columns incorporating strain-softening behavior of columns. International Journal of Geomechanics, 2015. 15(2): p. 04014047.

[4] Bilgin, Ö. and E. Mansour, Effect of reinforcement type on the design reinforcement length of

mechanically stabilized earth walls. Engineering Structures, 2014. 59: p. 663-673.

[5] Berg, R.R., NC. Samtani, and B.R. Christopher, Design of mechanically stabilized earth walls and reinforced soil slopes–Volume II. 2009, United States. Department of Transportation. Federal Highway Administration.

[6] Bathurst, R.J. and D.L. Walters. Lessons learned from full scale testing of geosynthetic reinforced soil retaining walls. in ISRM International Symposium. 2000. ISRM.

[7] Ashaari, Y., Aspects of the behaviour of reinforced earth walls. 1990.

[8] Bobet, A., Design of MSE walls for fully saturated conditions. 2002.

[9] Khaniki, A.K., Application of reinforced soil walls in coastal protection. 1995.

[10] Hakimelahi, N., et al., effect of woven geotextile reinforcement on mechanical behavior of calcareous sands. Case Studies in Construction Materials, 2023. 18: p. e02014.

[11] Krishnaswamy, N., K. Rajagopal, and GM Latha, Model studies on geocell supported embankments constructed over a soft clay foundation. Geotechnical testing journal, 2000. 23(1): p. 45-54.

[12] Madhavi Latha, G. and K. Rajagopal, Parametric finite element analyses of geocell-supported embankments. Canadian Geotechnical Journal, 2007. 44(8): p. 917-927.

[13] Ling, H.I. and H. Liu, Deformation analysis of reinforced soil retaining walls—simplistic versus sophisticated finite element analyses. Acta Geotechnica, 2009. 4: p. 203-213.

[14] Elshafey, M., M. Elnaggar, and AY Abdelaziz, Numerical investigation of quay walls reinforced with geosynthetic. Alexandria Engineering Journal, 2021. 60(2): p. 2303-2313.

[15] Nagtegaal, J.C., DM Parks, and J. Rice, On numerically accurate finite element solutions in the fully plastic range. Computer methods in applied mechanics and engineering, 1974. 4(2): p. 153-177.

[16] Rowe, R. and K.L. Soderman, Stabilization of very soft soils using high strength geosynthetics: the role of finite element analyses. Geotextiles and Geomembranes, 1987. 6(1-3): p. 53-80.

[17] Helwany, S., Applied soil mechanics with ABAQUS applications. 2007: John Wiley & Sons.

[18] Ambauen, S.J., Numerical simulation of mechanically stabilized earth walls for parametric evaluation of behavior under surcharge loading. 2014.

[19] Dietz, A.L., Finite Element Modeling of Geosynthetic Soil Reinforcement Over Shallow Buried Pipes. 2013.

[20] Strömblad, N., Modeling of soil and structure interaction subsea. 2014.

[21] Thaker, G., V. Pawar, and D. Desai. Comparative study on settlement analysis of shallow foundation for cohesive soil. in Proceedings of the Indian Geotechnical Conference 2019: IGC-2019 Volume V. 2021. Springer.

[22] Officials, T., Standard specifications for highway bridges. 2002: Aashto.

[23] McElroy, M.W., Three dimensional finite element modeling of stacked geotextile tubes for embankment stabilization. 2008, Lehigh University.

[24] Koura, H., E. Tolba, and E. Galal, Stability Analysis of Geotextile Reinforced Marine Causeways. Port-Said Engineering Research Journal, 2020. 24(2): p. 31-39.

[25] Adams, M., et al., Geosynthetic reinforced soil integrated bridge system interim implementation guide. 2012, Federal Highway Administration (US).